

Enhancement of the dielectron continuum in Au+Au collisions at $\sqrt{s_{NN}}=200$ GeV

S. Afanasiev,¹⁷ C. Aidala,⁷ N.N. Ajitanand,⁴³ Y. Akiba,^{37,38} J. Alexander,⁴³ A. Al-Jamel,³³ K. Aoki,^{23,37} L. Aphecetche,⁴⁵ R. Armendariz,³³ S.H. Aronson,³ R. Averbeck,⁴⁴ T.C. Awes,³⁴ B. Azmoun,³ V. Babintsev,¹⁴ A. Baldisseri,⁸ K.N. Barish,⁴ P.D. Barnes,²⁶ B. Bassalleck,³² S. Bathe,⁴ S. Batsouli,⁷ V. Baublis,³⁶ F. Bauer,⁴ A. Bazilevsky,³ S. Belikov,^{3,16} R. Bennett,⁴⁴ Y. Berdnikov,⁴⁰ M.T. Bjornrdal,⁷ J.G. Boissevain,²⁶ H. Borel,⁸ K. Boyle,⁴⁴ M.L. Brooks,²⁶ D.S. Brown,³³ D. Bucher,²⁹ H. Buesching,³ V. Bumazhnov,¹⁴ G. Bunce,^{3,38} J.M. Burward-Hoy,²⁶ S. Butsyk,⁴⁴ S. Campbell,⁴⁴ J.-S. Chai,¹⁸ S. Chernichenko,¹⁴ J. Chiba,¹⁹ C.Y. Chi,⁷ M. Chiu,⁷ I.J. Choi,⁵² T. Chujo,⁴⁹ V. Cianciolo,³⁴ C.R. Cleven,¹² Y. Cobigo,⁸ B.A. Cole,⁷ M.P. Comets,³⁵ P. Constantin,¹⁶ M. Csanád,¹⁰ T. Csörgő,²⁰ T. Dahms,⁴⁴ K. Das,¹¹ G. David,³ H. Delagrange,⁴⁵ A. Denisov,¹⁴ D. d'Enterria,⁷ A. Deshpande,^{38,44} E.J. Desmond,³ O. Dietzsch,⁴¹ A. Dion,⁴⁴ J.L. Drachenberg,¹ O. Drapier,²⁴ A. Drees,⁴⁴ A.K. Dubey,⁵¹ A. Durum,¹⁴ V. Dzhordzhadze,⁴⁶ Y.V. Efremenko,³⁴ J. Egdemir,⁴⁴ A. Enokizono,¹³ H. En'yo,^{37,38} B. Espagnon,³⁵ S. Esumi,⁴⁸ D.E. Fields,^{32,38} F. Fleuret,²⁴ S.L. Fokin,²² B. Forestier,²⁷ Z. Fraenkel,⁵¹ J.E. Frantz,⁷ A. Franz,³ A.D. Frawley,¹¹ Y. Fukao,^{23,37} S.-Y. Fung,⁴ S. Gadrat,²⁷ F. Gastineau,⁴⁵ M. Germain,⁴⁵ A. Glenn,⁴⁶ M. Gonin,²⁴ J. Gosset,⁸ Y. Goto,^{37,38} R. Granier de Cassagnac,²⁴ N. Grau,¹⁶ S.V. Greene,⁴⁹ M. Grosse Perdekamp,^{15,38} T. Gunji,⁵ H.-Å. Gustafsson,²⁸ T. Hachiya,^{13,37} A. Hadj Henni,⁴⁵ J.S. Haggerty,³ M.N. Hagiwara,¹ H. Hamagaki,⁵ H. Harada,¹³ E.P. Hartouni,²⁵ K. Haruna,¹³ M. Harvey,³ E. Haslum,²⁸ K. Hasuko,³⁷ R. Hayano,⁵ M. Heffner,²⁵ T.K. Hemmick,⁴⁴ J.M. Heuser,³⁷ X. He,¹² H. Hiejima,¹⁵ J.C. Hill,¹⁶ R. Hobbs,³² M. Holmes,⁴⁹ W. Holzmann,⁴³ K. Homma,¹³ B. Hong,²¹ T. Horaguchi,^{37,47} M.G. Hur,¹⁸ T. Ichihara,^{37,38} K. Imai,^{23,37} M. Inaba,⁴⁸ D. Isenhower,¹ L. Isenhower,¹ M. Ishihara,³⁷ T. Isobe,⁵ M. Issah,⁴³ A. Isupov,¹⁷ B.V. Jacak,^{44,*} J. Jia,⁷ J. Jin,⁷ O. Jinnouchi,³⁸ B.M. Johnson,³ K.S. Joo,³⁰ D. Jouan,³⁵ F. Kajihara,^{5,37} S. Kametani,^{5,50} N. Kamihara,^{37,47} M. Kaneta,³⁸ J.H. Kang,⁵² T. Kawagishi,⁴⁸ A.V. Kazantsev,²² S. Kelly,⁶ A. Khanzadeev,³⁶ D.J. Kim,⁵² E. Kim,⁴² Y.-S. Kim,¹⁸ E. Kinney,⁶ A. Kiss,¹⁰ E. Kistenev,³ A. Kiyomichi,³⁷ C. Klein-Boesing,²⁹ L. Kochenda,³⁶ V. Kochetkov,¹⁴ B. Komkov,³⁶ M. Konno,⁴⁸ D. Kotchetkov,⁴ A. Kozlov,⁵¹ P.J. Kroon,³ G.J. Kunde,²⁶ N. Kurihara,⁵ K. Kurita,^{39,37} M.J. Kweon,²¹ Y. Kwon,⁵² G.S. Kyle,³³ R. Lacey,⁴³ J.G. Lajoie,¹⁶ A. Lebedev,¹⁶ Y. Le Bornec,³⁵ S. Leckey,⁴⁴ D.M. Lee,²⁶ M.K. Lee,⁵² M.J. Leitch,²⁶ M.A.L. Leite,⁴¹ H. Lim,⁴² A. Litvinenko,¹⁷ M.X. Liu,²⁶ X.H. Li,⁴ C.F. Maguire,⁴⁹ Y.I. Makdisi,³ A. Malakhov,¹⁷ M.D. Malik,³² V.I. Manko,²² H. Masui,⁴⁸ F. Matathias,⁴⁴ M.C. McCain,¹⁵ P.L. McGaughey,²⁶ Y. Miake,⁴⁸ T.E. Miller,⁴⁹ A. Milov,⁴⁴ S. Mioduszewski,³ G.C. Mishra,¹² J.T. Mitchell,³ D.P. Morrison,³ J.M. Moss,²⁶ T.V. Moukhanova,²² D. Mukhopadhyay,⁴⁹ J. Murata,^{39,37} S. Nagamiya,¹⁹ Y. Nagata,⁴⁸ J.L. Nagle,⁶ M. Naglis,⁵¹ T. Nakamura,¹³ J. Newby,²⁵ M. Nguyen,⁴⁴ B.E. Norman,²⁶ A.S. Nyanin,²² J. Nystrand,²⁸ E. O'Brien,³ C.A. Ogilvie,¹⁶ H. Ohnishi,³⁷ I.D. Ojha,⁴⁹ H. Okada,^{23,37} K. Okada,³⁸ O.O. Omiwade,¹ A. Oskarsson,²⁸ I. Otterlund,²⁸ K. Ozawa,⁵ D. Pal,⁴⁹ A.P.T. Palounek,²⁶ V. Pantuev,⁴⁴ V. Papavassiliou,³³ J. Park,⁴² W.J. Park,²¹ S.F. Pate,³³ H. Pei,¹⁶ J.-C. Peng,¹⁵ H. Pereira,⁸ V. Peresedov,¹⁷ D.Yu. Peressounko,²² C. Pinkenburg,³ R.P. Pisani,³ M.L. Purschke,³ A.K. Purwar,⁴⁴ H. Qu,¹² J. Rak,¹⁶ I. Ravinovich,⁵¹ K.F. Read,^{34,46} M. Reuter,⁴⁴ K. Reygers,²⁹ V. Riabov,³⁶ Y. Riabov,³⁶ G. Roche,²⁷ A. Romana,^{24,†} M. Rosati,¹⁶ S.S.E. Rosendahl,²⁸ P. Rosnet,²⁷ P. Rukoyatkin,¹⁷ V.L. Rykov,³⁷ S.S. Ryu,⁵² B. Sahlmueller,²⁹ N. Saito,^{23,37,38} T. Sakaguchi,^{5,50} S. Sakai,⁴⁸ V. Samsonov,³⁶ H.D. Sato,^{23,37} S. Sato,^{3,19,48} S. Sawada,¹⁹ V. Semenov,¹⁴ R. Seto,⁴ D. Sharma,⁵¹ T.K. Shea,³ I. Shein,¹⁴ T.-A. Shibata,^{37,47} K. Shigaki,¹³ M. Shimomura,⁴⁸ T. Shohjoh,⁴⁸ K. Shoji,^{23,37} A. Sickles,⁴⁴ C.L. Silva,⁴¹ D. Silvermyr,³⁴ K.S. Sim,²¹ C.P. Singh,² V. Singh,² S. Skutnik,¹⁶ W.C. Smith,¹ A. Soldatov,¹⁴ R.A. Soltz,²⁵ W.E. Sondheim,²⁶ S.P. Sorensen,⁴⁶ I.V. Sourikova,³ F. Staley,⁸ P.W. Stankus,³⁴ E. Stenlund,²⁸ M. Stepanov,³³ A. Ster,²⁰ S.P. Stoll,³ T. Sugitate,¹³ C. Suire,³⁵ J.P. Sullivan,²⁶ J. Sziklai,²⁰ T. Tabaru,³⁸ S. Takagi,⁴⁸ E.M. Takagui,⁴¹ A. Taketani,^{37,38} K.H. Tanaka,¹⁹ Y. Tanaka,³¹ K. Tanida,^{37,38} M.J. Tannenbaum,³ A. Taranenko,⁴³ P. Tarján,⁹ T.L. Thomas,³² M. Togawa,^{23,37} A. Toia,⁴⁴ J. Tojo,³⁷ H. Torii,³⁷ R.S. Towell,¹ V.-N. Tram,²⁴ I. Tserruya,⁵¹ Y. Tsuchimoto,^{13,37} S.K. Tuli,² H. Tydesjö,²⁸ N. Tyurin,¹⁴ H. Valle,⁴⁹ H.W. vanHecke,²⁶ J. Velkovska,⁴⁹ R. Vertesi,⁹ A.A. Vinogradov,²² E. Vznuzdaev,³⁶ M. Wagner,^{23,37} X.R. Wang,³³ Y. Watanabe,^{37,38} J. Wessels,²⁹ S.N. White,³ N. Willis,³⁵ D. Winter,⁷ C.L. Woody,³ M. Wysocki,⁶ W. Xie,^{4,38} A. Yanovich,¹⁴ S. Yokkaichi,^{37,38} G.R. Young,³⁴ I. Younus,³² I.E. Yushmanov,²² W.A. Zajc,⁷ O. Zaudtke,²⁹ C. Zhang,⁷ J. Zimányi,^{20,†} and L. Zolin¹⁷

(PHENIX Collaboration)

¹Abilene Christian University, Abilene, TX 79699, U.S.

²Department of Physics, Banaras Hindu University, Varanasi 221005, India

³Brookhaven National Laboratory, Upton, NY 11973-5000, U.S.

- ⁴University of California - Riverside, Riverside, CA 92521, U.S.
- ⁵Center for Nuclear Study, Graduate School of Science, University of Tokyo, 7-3-1 Hongo, Bunkyo, Tokyo 113-0033, Japan
- ⁶University of Colorado, Boulder, CO 80309, U.S.
- ⁷Columbia University, New York, NY 10027 and Nevis Laboratories, Irvington, NY 10533, U.S.
- ⁸Dapnia, CEA Saclay, F-91191, Gif-sur-Yvette, France
- ⁹Debrecen University, H-4010 Debrecen, Egyetem tér 1, Hungary
- ¹⁰ELTE, Eötvös Loránd University, H - 1117 Budapest, Pázmány P. s. 1/A, Hungary
- ¹¹Florida State University, Tallahassee, FL 32306, U.S.
- ¹²Georgia State University, Atlanta, GA 30303, U.S.
- ¹³Hiroshima University, Kagamiyama, Higashi-Hiroshima 739-8526, Japan
- ¹⁴IHEP Protvino, State Research Center of Russian Federation, Institute for High Energy Physics, Protvino, 142281, Russia
- ¹⁵University of Illinois at Urbana-Champaign, Urbana, IL 61801, U.S.
- ¹⁶Iowa State University, Ames, IA 50011, U.S.
- ¹⁷Joint Institute for Nuclear Research, 141980 Dubna, Moscow Region, Russia
- ¹⁸KAERI, Cyclotron Application Laboratory, Seoul, South Korea
- ¹⁹KEK, High Energy Accelerator Research Organization, Tsukuba, Ibaraki 305-0801, Japan
- ²⁰KFKI Research Institute for Particle and Nuclear Physics of the Hungarian Academy of Sciences (MTA KFKI RMKI), H-1525 Budapest 114, POBox 49, Budapest, Hungary
- ²¹Korea University, Seoul, 136-701, Korea
- ²²Russian Research Center "Kurchatov Institute", Moscow, Russia
- ²³Kyoto University, Kyoto 606-8502, Japan
- ²⁴Laboratoire Leprince-Ringuet, Ecole Polytechnique, CNRS-IN2P3, Route de Saclay, F-91128, Palaiseau, France
- ²⁵Lawrence Livermore National Laboratory, Livermore, CA 94550, U.S.
- ²⁶Los Alamos National Laboratory, Los Alamos, NM 87545, U.S.
- ²⁷LPC, Université Blaise Pascal, CNRS-IN2P3, Clermont-Fd, 63177 Aubiere Cedex, France
- ²⁸Department of Physics, Lund University, Box 118, SE-221 00 Lund, Sweden
- ²⁹Institut für Kernphysik, University of Muenster, D-48149 Muenster, Germany
- ³⁰Myongji University, Yongin, Kyonggido 449-728, Korea
- ³¹Nagasaki Institute of Applied Science, Nagasaki-shi, Nagasaki 851-0193, Japan
- ³²University of New Mexico, Albuquerque, NM 87131, U.S.
- ³³New Mexico State University, Las Cruces, NM 88003, U.S.
- ³⁴Oak Ridge National Laboratory, Oak Ridge, TN 37831, U.S.
- ³⁵IPN-Orsay, Université Paris Sud, CNRS-IN2P3, BP1, F-91406, Orsay, France
- ³⁶PNPI, Petersburg Nuclear Physics Institute, Gatchina, Leningrad region, 188300, Russia
- ³⁷RIKEN, The Institute of Physical and Chemical Research, Wako, Saitama 351-0198, Japan
- ³⁸RIKEN BNL Research Center, Brookhaven National Laboratory, Upton, NY 11973-5000, U.S.
- ³⁹Physics Department, Rikkyo University, 3-34-1 Nishi-Ikebukuro, Toshima, Tokyo 171-8501, Japan
- ⁴⁰Saint Petersburg State Polytechnic University, St. Petersburg, Russia
- ⁴¹Universidade de São Paulo, Instituto de Física, Caixa Postal 66318, São Paulo CEP05315-970, Brazil
- ⁴²System Electronics Laboratory, Seoul National University, Seoul, South Korea
- ⁴³Chemistry Department, Stony Brook University, Stony Brook, SUNY, NY 11794-3400, U.S.
- ⁴⁴Department of Physics and Astronomy, Stony Brook University, SUNY, Stony Brook, NY 11794, U.S.
- ⁴⁵SUBATECH (Ecole des Mines de Nantes, CNRS-IN2P3, Université de Nantes) BP 20722 - 44307, Nantes, France
- ⁴⁶University of Tennessee, Knoxville, TN 37996, U.S.
- ⁴⁷Department of Physics, Tokyo Institute of Technology, Oh-okayama, Meguro, Tokyo 152-8551, Japan
- ⁴⁸Institute of Physics, University of Tsukuba, Tsukuba, Ibaraki 305, Japan
- ⁴⁹Vanderbilt University, Nashville, TN 37235, U.S.
- ⁵⁰Waseda University, Advanced Research Institute for Science and Engineering, 17 Kikui-cho, Shinjuku-ku, Tokyo 162-0044, Japan
- ⁵¹Weizmann Institute, Rehovot 76100, Israel
- ⁵²Yonsei University, IPAP, Seoul 120-749, Korea

(Dated: February 1, 2008)

The PHENIX experiment has measured the dielectron continuum in $\sqrt{s_{NN}}=200$ GeV Au+Au collisions. In minimum bias collisions the dielectron yield in the mass range between 150 and 750 MeV/c² is enhanced by a factor of $3.4 \pm 0.2(\text{stat.}) \pm 1.3(\text{syst.}) \pm 0.7(\text{model})$ compared to the expectation from our model of hadron decays. The integrated yield increases faster with the centrality of the collisions than the number of participating nucleons, suggesting emission from scattering processes in the hot and dense medium. The continuum yield between the masses of the ϕ and the J/ψ mesons is consistent with expectations from correlated $c\bar{c}$ production, though other mechanisms are not ruled out.

PACS numbers: 25.75.Dw

Electron-positron pairs, or dileptons in general, have proven to be an excellent tool to study collisions of heavy ions at ultra-relativistic energies. Because leptons do not interact strongly, emission of dileptons from the hot matter created at RHIC should leave an imprint on the observed dilepton distributions. Emission from the hot matter may include thermal radiation and in-medium decays of mesons with short lifetimes, like the ρ meson, while their spectral functions may be strongly modified. However, below the mass of the ϕ meson, these sources compete with a large contribution of e^+e^- -pairs from Dalitz decays of pseudoscalar mesons (π^0, η, η') and decays of vector mesons (ρ, ω, ϕ). Above the ϕ meson mass up to 4.5 GeV/c², competing sources are dilepton decays of charmonia ($J/\psi, \psi'$) and semileptonic decays of D and \bar{D} mesons, correlated through flavor conservation, which lead to a continuum of masses. In addition to thermal radiation, energy loss of charm quarks in the medium might modify the continuum yield in this mass region.

The discovery of a large enhancement of the dilepton yield at masses below the ϕ meson mass in ion-ion collisions at the CERN SPS [1] has triggered a broad theoretical investigation of modifications of properties of hadrons in a dense medium and of how these modifications relate to chiral symmetry restoration [2]. These theoretical studies will benefit from the availability of more precise data from CERN [3, 4] and GSI [5]. An enhanced yield was also observed at higher masses, above the ϕ meson mass [6]. Recent NA60 data suggest that the enhancement can not be attributed to decays of D-mesons but may result from prompt production, as expected for thermal radiation [7].

The PHENIX experiment at the Relativistic Heavy Ion Collider (RHIC) extends these measurements in a new energy regime by exploring Au+Au collisions at a center of mass energy of $\sqrt{s_{NN}}=200$ GeV. In this paper we present results from minimum bias data taken in 2004. Collisions were triggered and selected by centrality using beam-beam counters (BBC) and zero degree calorimeters (ZDC). We analyzed a sample of 8×10^8 minimum bias events.

Electrons and positrons are reconstructed in the two central arm spectrometers of PHENIX [8] using Drift Chambers (DC), located outside an axial magnetic field, which measure their momenta with an accuracy of $\sigma_p/p = 0.7\% \oplus 1\% p/(\text{GeV}/c)$. They are identified by hits in the Ring Imaging Cherenkov detector (RICH) and by matching the momentum with the energy measured in an electromagnetic calorimeter (EMCal) [9]. Electrons are reconstructed with an efficiency of $\sim 90\%$, while a hadron contamination of $\sim 20\%$ remains.

Each central arm covers $|\Delta\eta| \leq 0.35$ in pseudorapidity and $\pi/2$ in azimuthal angle. Because charged particles are deflected in the azimuthal direction by the magnetic field, the acceptance depends on the momentum and the charge of the particle, and also on the radial location of

the detector component (DC, EMCal and RICH). The acceptance for a track with charge q , transverse momentum p_T and azimuthal emission angle ϕ can be described by:

$$\phi_{\min} \leq \phi + q \frac{k_{\text{DC,RICH}}}{p_T} \leq \phi_{\max} \quad (1)$$

where k_{DC} and k_{RICH} represent the effective azimuthal bend to DC and RICH ($k_{\text{DC}} = 0.206$ rad GeV/c and $k_{\text{RICH}} = 0.309$ rad GeV/c). One arm has $\phi_{\min} = \frac{-3}{16}\pi$ and $\phi_{\max} = \frac{5}{16}\pi$, the other arm $\phi_{\min} = \frac{11}{16}\pi$ and $\phi_{\max} = \frac{19}{16}\pi$. Only electrons with $p_T \geq 200$ MeV/c are used in the analysis. The photon conversion probability was minimized by installing a helium bag between the beam pipe and the DC, reducing the material to $\sim 0.4\%$ of a radiation length.

In an event the source of any electron or positron is unknown and therefore all electrons and positrons are combined to pairs, like-sign and unlike-sign. This results in a large combinatorial background which must be removed. The background is computed with a mixed event technique, which combines tracks from different events that have similar topology (centrality, collision vertex, reaction plane).

In order to achieve the necessary accuracy, all unphysical correlations that arise from overlapping tracks or hits in the detectors, mostly in the RICH, must be eliminated, because they can not be reproduced by mixed events. If hits of both tracks of a pair overlap in any detector, the event is rejected. About 4% of all pairs are removed by this event rejection. Comparing measured like-sign pairs with the mixed combinatorial background shows that the mixing technique reproduces the shape within the statistical accuracy of the data.

The absolute normalization of the unlike-sign combinatorial background is given by the geometrical mean of the observed positive and negative like-sign pairs $2\sqrt{N_{--}N_{++}}$, where, in principle, N_{--} and N_{++} are the measured number of like-sign pairs. There is a small correlated signal also in the observed like-sign pairs, which can occur if there are two e^+e^- -pairs in the final state of a meson, e.g. double Dalitz decays, Dalitz decays followed by a conversion of the decay photon or two photon decays followed by conversion of both photons. These “cross” pairs have small masses, typically less than the η mass (550 MeV/c²).

We therefore determine N_{--} and N_{++} by integrating the mixed event distributions after they were normalized to the 7.5×10^6 like-sign pairs measured above 700 MeV/c². N_{--} and N_{++} are determined with an accuracy of 0.12%. The normalization is multiplied by 1.004 to account for the fact that the event rejection removes 10% more like-sign than unlike-sign pairs. This correction factor was estimated, using mixed events, with an accuracy better than 50%. Adding the statistical error

and the uncertainty due to the event rejection in quadrature gives an accuracy of 0.25% on the normalization.

After subtraction of the combinatorial background, physical background from photon conversions and cross pairs is removed. Because the tracking assumes that the e^+e^- -pair originates at the collision vertex, pairs from photons that convert in or outside of the beampipe are reconstructed with finite mass and opening angle, which is oriented perpendicular to the magnetic field. A cut on the orientation of the opening angle in the field removes more than 98% of the conversion pairs.

Cross pairs occur as like and unlike-sign pairs. Monte Carlo simulations show that the rate of unlike-sign cross pairs accepted in PHENIX is 44% of the rate for like-sign cross pairs. To determine the rate of unlike-sign cross pairs, we scale the simulated like-sign cross pair distribution to the observed like-sign signal, obtained by subtraction of the mixed event background normalized above 700 MeV/c². We note that the like-sign signal is well described by the Monte Carlo simulation. The simulated unlike-sign cross pair distribution is scaled by the same factor and subtracted from the unlike-sign signal. The uncertainty of this subtraction depends on mass, but is $\leq 9\%$ of the final yield.

Figure 1 shows the mass distribution of e^+e^- -pairs, the normalized mixed event background (B), and the signal yield (S) obtained by subtracting the mixed event background, the cross pairs and the conversion pairs. The insert shows the signal-to-background ratio (S/B). The systematic errors (boxes) reflect the error on the background subtraction, which is given by $\delta_S/S = 0.25\% \cdot B/S$, added in quadrature to the uncertainty due to the cross pair subtraction, assumed to be $9\%S$ below 600 MeV/c². Despite the small S/B ratio, the vector meson resonances ω , ϕ and J/ψ which decay directly to e^+e^- , and an e^+e^- -pair continuum is visible up to 4.5 GeV/c².

In order to check the background subtraction, a subset of data (5×10^7 events), taken with additional material wrapped around the beam pipe to increase the number of photon conversions [9], was analyzed. In this data set the combinatorial background and the cross pair contribution is larger by a factor of ~ 2.5 . As shown in Fig. 1, the results from both data sets agree well within statistical errors, which are 30% in the range from 150 to 750 MeV/c² and much less below. Considering the decreased S/B ratio for the data with the converter we can estimate a 0.1% scale uncertainty of the background normalization, well within the 0.25% systematic uncertainty assigned.

The spectra are corrected to represent the invariant yield of e^+e^- -pairs, with both the e^+ and e^- in the detector acceptance as specified in Eq. 1. The correction is determined using a GEANT simulation [10] of the PHENIX detector that includes the details of the detector response. Simulated e^+e^- -pairs are reconstructed

with the same analysis chain and all cuts applied. The correction is determined double differentially in p_T and mass of the e^+e^- -pair. The reduction of the electron reconstruction efficiency (0.92 ± 0.03) due to detector occupancy is corrected for. Systematic uncertainties on the correction can be summarized as: (i) 13.4% on dielectron reconstruction, which is twice the uncertainty on the electron reconstruction efficiency [9], (ii) 6% conversion rejection cut, (iii) 5% event rejection and (iv) 3% occupancy. These uncertainties are included in the final systematic error on the invariant e^+e^- -pair yield.

Figure 2 compares the invariant yield to the expected yield from meson decays and correlated decays of charmed mesons. The cocktail of hadron decay contributions was estimated using PHENIX data for meson production when available. As input distributions we use the measured π , η , ϕ , J/ψ yield and spectra [11, 12, 13, 14, 15]. For other mesons we use the m_T scaling procedure outlined in [9]. The systematic uncertainties depend on mass and range from 10 to 25%.

For the continuum below the J/ψ the dynamic correlation of c and \bar{c} is essential, but unknown. We make two assumptions: (i) the correlation is unchanged by the medium and equal to what is known from p+p collisions. In this case we use PYTHIA [16] scaled from the p+p equivalent $c\bar{c}$ cross section of $567 \pm 57 \pm 193 \mu\text{barn}$ [17] to minimum bias Au+Au collisions proportional to the number of binary collisions (258 ± 25) [12]. We note that the p_T distribution for electrons generated by PYTHIA is softer than the spectra measured in p+p data but coincides with those observed in Au+Au [9]. As a second assumption (ii) there is no dynamical correlation, i.e. the direction of c and \bar{c} quarks are uncorrelated. We keep the overall cross section and the p_T distributions fixed to experimental data [9]. Other contributions from bottom and Drell-Yan are expected to be small in the mass region below the J/ψ peak. Each e^+ and e^- must fall in the PHENIX acceptance, given by Eq. 1.

The data below 150 MeV/c² are well described by the cocktail of hadronic sources. The vector mesons ω , ϕ and J/ψ are reproduced within the uncertainties. However, the yield is substantially enhanced above the expected yield in the continuum region from 150 to 750 MeV/c². The enhancement in this mass range is a factor of $3.4 \pm 0.2(\text{stat.}) \pm 1.3(\text{syst.}) \pm 0.7(\text{model})$, where the first error is the statistical error, the second the systematic uncertainty of the data, and the last error is an estimate of the uncertainty of the expected yield. Above the ϕ meson mass the data seem to be well described by the continuum calculation based on PYTHIA. This is somewhat surprising, since single electron distributions from charm show substantial medium modifications [9], and thus it is hard to understand how the dynamic correlation at production of the $c\bar{c}$ remains unaffected by the medium. A complete randomization of that correlation (see Fig.2) leads to a much softer mass spectrum and

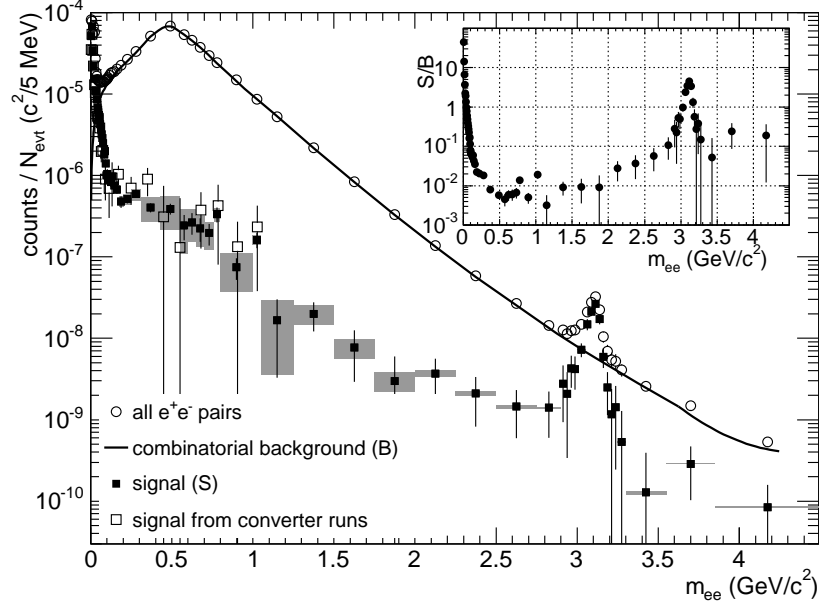


FIG. 1: Uncorrected mass spectra of all e^+e^- pairs, mixed events background (B) and signal (S) with statistical (bars) and systematic (boxes) uncertainties shown separately. The signal from the runs with additional converter is shown with statistical errors only. The insert shows the S/B ratio. The mass range covered by each data point is given by horizontal bars.

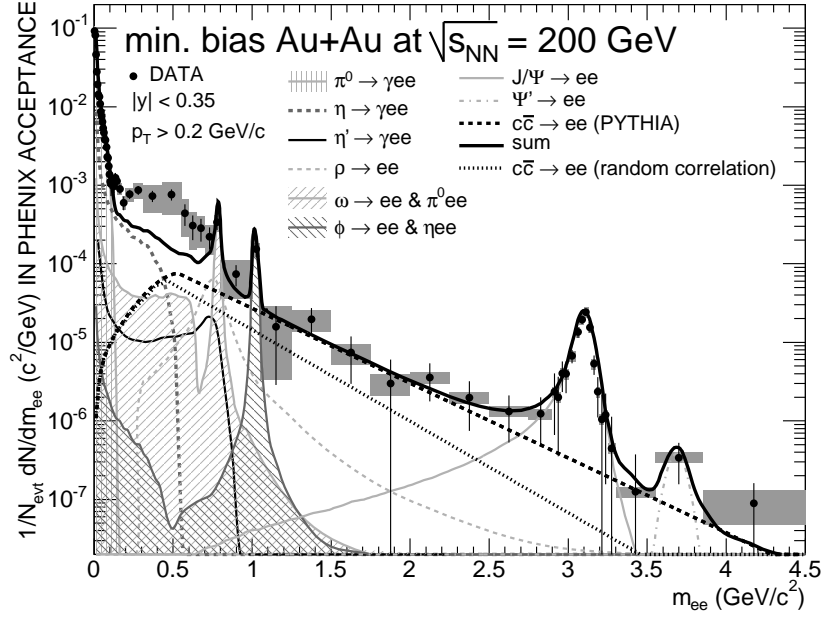


FIG. 2: Invariant e^+e^- -pair yield compared to the yield from the model of hadron decays. The charmed meson decay contribution based on PYTHIA is included in the sum of sources (solid black line). The charm contribution expected if the dynamic correlation of c and \bar{c} is removed is shown separately. Statistical (bars) and systematic (boxes) uncertainties are shown separately; the mass range covered by each data point is given by horizontal bars. The systematic uncertainty on the cocktail is not shown.

would leave significant room for other contributions, e.g. thermal radiation.

To shed more light on the continuum yield we have studied the centrality dependence of the yield in three mass windows, below 100 MeV/c², from 150 to 750

MeV/c² and 1.2 to 2.8 GeV/c². The top panel of Fig. 3 shows the centrality dependence of the yield in the mass region 150–750 MeV/c² divided by the number of participating nucleon pairs ($N_{\text{part}}/2$). For comparison the yield below 100 MeV/c², which is dominated by low p_T

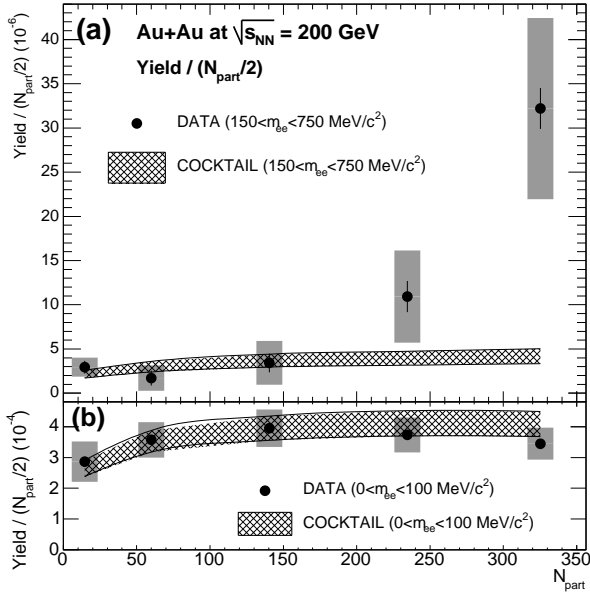


FIG. 3: Dielectron yield per participating nucleon pairs ($N_{\text{part}}/2$) as function of N_{part} for two different mass ranges compared to the expected yield from the hadron decay model. The two lines give $\pm 1\sigma$ systematic uncertainty. For the data statistical and systematic uncertainties are shown separately.

pion decays, is shown in the lower panel. For both intervals the yield is compared to the same yield calculated from the hadron cocktail. In the lower mass range the yield agrees with the expectation, i.e. is proportional to the pion yield. In contrast, in the range from 150 to 750 MeV/ c^2 , the observed yield rises significantly compared to the expectation, reaching a factor of $7.7 \pm 0.6(\text{stat.}) \pm 2.5(\text{syst.}) \pm 1.5(\text{model})$ for most central collisions. The increase is qualitatively consistent with the conjecture that an in-medium enhancement of the dielectron continuum yield arises from scattering processes like $\pi\pi$ or $q\bar{q}$ annihilation, which would result in a yield rising faster than proportional to N_{part} .

We normalize the yield in the mass region 1.2 to 2.8 GeV/ c^2 to the number of binary collisions (Fig. 4), which is the correct scaling for pairs from charmed meson decays [9]. The normalized yield shows no significant centrality dependence and is consistent with the expectation based on PYTHIA. It is also likely that a scenario where the correlation between the c and \bar{c} is randomized will require an additional source, e.g. a contribution from thermal radiation. This contribution could increase faster than linear with N_{part} and therefore the apparent scaling with N_{coll} may be a mere coincidence. We note that this coincidence may have been observed in this mass region at the CERN SPS [6], where a major prompt component has now been suggested by NA60 data [7].

In conclusion, measurements of Au+Au collisions at $\sqrt{s_{NN}}=200$ GeV in the mass range 150–750 MeV/ c^2

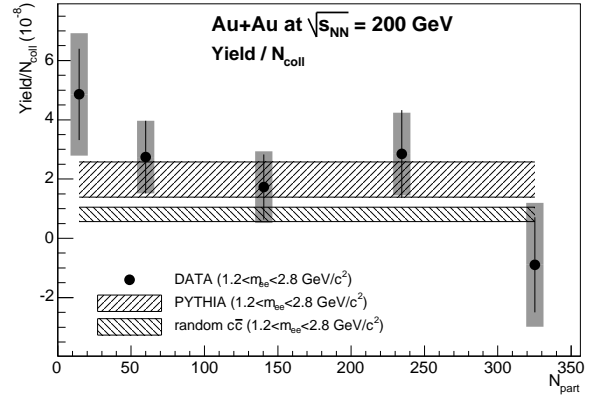


FIG. 4: Dielectron yield per number of collisions N_{coll} in the mass range 1.2 to 2.8 GeV/ c^2 as function of N_{part} . Statistical and systematic errors are shown separately. Also shown are two bands corresponding to the two different estimates of the contribution from charmed meson decays. The width of the band reflect the uncertainty of the charm cross-section only.

show a significant enhancement of the dielectron continuum and exhibit a clear increase with centrality of the collision. The observed yield between ϕ and J/ψ is consistent with the expectation from correlated $c\bar{c}$ production, but does not exclude other mechanisms.

We thank the staff of the Collider-Accelerator and Physics Departments at BNL for their vital contributions. We acknowledge support from the Office of Nuclear Physics in DOE Office of Science and NSF (U.S.A.), MEXT and JSPS (Japan), CNPq and FAPESP (Brazil), NSFC (China), IN2P3/CNRS, and CEA (France), BMBF, DAAD, and AvH (Germany), OTKA (Hungary), DAE (India), ISF (Israel), KRF and KOSEF (Korea), MES, RAS, and FAE (Russia), VR and KAW (Sweden), U.S. CRDF for the FSU, US-Hungarian NSF-OTKA-MTA, and US-Israel BSF.

* PHENIX Spokesperson: jacak@skipper.physics.sunysb.edu

† Deceased

- [1] G. Agakishiev *et al.*, Phys.Rev.Lett.75 1272 (1995)
- [2] R. Rapp, J.Wambach, Adv.Nucl.Phys. 25 1 (2000) and references therein
- [3] G.Agakishiev *et al.*, Eur.Phys.J. C 41 475 (2005)
- [4] R. Arnaldi *et al.*, Phys. Rev. Lett. **96**, 162302 (2006)
- [5] G. Agakishiev, Phys. Rev. Lett. **98**, 052302 (2007)
- [6] M.C. Abreu *et al.*, Eur. Phys. J. C **14**, 443 (2000).
- [7] R. Shahoian *et al.*, PoS **HEP2005**, 131 (2006).
- [8] K. Adcox *et al.*, Nucl. Instr. and Meth. A **A499**, 469 (2003).
- [9] A. Adare *et al.*, Phys. Rev. Lett. **98**, 172301 (2007)
- [10] GEANT User's Guide, 3.15, CERN Program Library
- [11] A. Adare *et al.*, Phys. Rev. Lett. **98**, 232301 (2007)
- [12] S. S. Adler *et al.*, Phys. Rev. C **69**, 034909 (2004)

- [13] S. S. Adler *et al.*, Phys. Rev. Lett. **91**, 072301 (2003)
- [14] S. S. Adler *et al.*, Phys. Rev. C **75**, 024909 (2007)
- [15] S. S. Adler *et al.*, Phys. Rev. C **72**, 014903 (2005)
- [16] We used PYTHIA 6.152 with parameters as in K. Adcox
et al., Phys. Rev. Lett. **88**, 192303 (2002)
- [17] A. Adare *et al.* Phys. Rev. Lett. **97**, 252002 (2006)